© 2006

EFFECTS OF DISORDER ON THE RAMAN LINE SHAPE IN ZrO$_2$

L. A. Falkovsky [*]

Landau Institute for Theoretical Physics
119337, Moscow, Russia

Experimental data obtained by Lughi and Clarke [5] are compared to the theory describing disorder effects on optical phonons. Sharpening and vanishing of the asymmetry of the Raman lines after annealing are attributed to a decrease in short-range disorder. The parameters of disorder (such as the phonon–defect coupling and the correlation length) are defined in the comparison.

PACS: 63.50.+x, 78.30.-j

1. INTRODUCTION

Raman scattering has been used for years to measure the center-zone phonon frequencies. But it was understood quite recently that studies of the Raman line shape can also provide widespread information relative to disorder, for instance, the isotopic compositions [1], the stacking faults [2, 3], the strain fluctuations near interfaces [4]. The phonon scattering processes by defects of various types result in increasing the phonon relaxation rate and consequently the Raman line width.

A novel field of Raman spectroscopy, the transformation kinetics, was put forward by Lughi and Clarke [5]. They investigated the phase transformations of yttria-stabilized zirconia. Zirconia ZnO$_2$ has a wide range of applications, including traditional structural refractories, fuel cells, and electronic devices such as oxygen sensors. Because of these technological implications, the characterization of zirconia is of particular interest. Zirconia has three zero-pressure polymorphs: the high-temperature cubic (c) phase (stable between 2570 K and the melting temperature 2980 K), the tetragonal (t) phase (stable between 1400 and 2570 K), and monoclinic (m) phase below 1400 K.

The unit cell of the c phase contains one formula unit. There is only one triply degenerated Raman-active mode at 640 cm^{-1} [6, 7]. From the symmetry analysis, it is suggested [8, 9] that the c–t transformation of ZnO$_2$ results from a condensation of the Brillouin zone boundary phonons. Indeed, it was found in

the model calculation [10, 11] of phonon curves that the phonon frequency $\omega(X_2^-)$ of the c phase is close to zero. The volume of the elementary cell is doubled in the c–t transformation. In the t phase, there are six Raman-active modes [12, 13] (their frequencies are given below in Table).

In paper [5], zirconia coatings were obtained by electron-beam evaporation and then annealed. The X-ray diffraction and Raman spectroscopy measurements were performed before and after annealing. They give a possibility to control the phase transformation in the samples. The obtained results are very interesting because they demonstrate the gigantic effect of annealing on both the width and asymmetry of the Raman line.

In the present paper, we compare the results obtained in Ref. [5] with the theory [14] describing the disorder effect on the optical phonons. A sketch of the theory is presented in Sec. 2. The comparison of the theory with the experiment [5] are given in Sec. 3. In Sec. 4, concluding remarks are summarized.

2. THEORETICAL BACKGROUND: PHONON ELASTIC SCATTERING BY STATIC DISORDER

The scattering of phonons by disorder (defects or strain fluctuations) results in the phonon width and shift (see [15] for a review). To estimate the effect of disorder, we can use the quantum mechanical for-

[*]E-mail: falk@itp.ac.ru

177

Final values obtained in fitting for spectra from the samples after annealing at 1200 °C (Ann) and as deposited (Asd): the experimental [13] phonon frequency Ω_{exp}, the peak position Ω_0, the peak position ω_0 including only the homogeneous shift, the total line width Γ_0 (subscript «0» is referred to as the peak position), the natural line width Γ^{nat}, the line asymmetry As, the interaction parameter A (all in cm^{-1}), the defect radius r_0/a (dimensionless), the relative intensity I_0, and the type of extremum

Line	Ω_{exp}	Ω_0	ω_0	Γ_0	Γ^{nat}	As	A	r_0/a	I_0	Extr. type
1 Ann	149	148.6	148.6	8.7	8.7	0	0	—	0.215	min
1 Asd		151.2	152.0	14.6	8.7	3.1	225	1.60	0.19	min
2 Ann	269	264.0	264.0	25.5	25.5	0	0	—	3.32	max
2 Asd		250.9	245.0	48.0	25.5	−23.7	225	0.73	2.55	max
3 Ann	319	321.0	321.0	26.0	26.0	0	0	—	1.15	max
3 Asd		330.4	325.0	45.0	26.0	−18.4	200	0.83	1.10	max
4 Ann	461	463.3	463.3	20.0	20.0	0	0	—	1.55	min
4 Asd		470.5	472.5	26.5	20.0	5.2	100	1.27	1.45	min
5 Ann	602	604.5	604.5	36.0	36.0	0	0	—	3.30	min
5 Asd		602.1	605.0	43.3	36.0	5.8	75	0.95	2.30	min
6 Ann	648	643.0	643.0	22.0	22.0	0	0	—	6.70	max
6 Asd		636.4	633.5	27.2	22.0	−3.9	50	0.95	7.85	max

mula [16]

$$\Gamma(\omega, \mathbf{q}) - \Gamma^{nat} \propto$$
$$\propto \pi c_d \sum_{\mathbf{k}} |v(\mathbf{k} - \mathbf{q})|^2 \delta(\omega_0^2 \pm s^2 k^2 - \omega^2), \quad (1)$$

giving the phonon width as a function of the frequency and wave vector. Here, c_d is the concentration of defects, $v(\mathbf{k} - \mathbf{q})$ is the phonon–defect interaction, ω is the phonon frequency in the initial state, $\omega_0^2 \pm s^2 k^2$ is the squared phonon frequency in the final state (the «+» sign if the phonon branch has a minimum at ω_0 and the «−» sign if there is a maximum), s is a dispersion parameter, and $\delta(x)$ is the Dirac δ-function, expressing the conservation law in the phonon elastic scattering. The summation is performed over the three-dimensional wave vector $\mathbf{k}$ in the case of phonon scattering by point defects under consideration.

We consider the short-range defects, with the interaction having the form of a δ-function in the real space. Then, the potential v is independent of the wave vector, i. e., $v(\mathbf{k} - \mathbf{q}) = v_0$ with a constant value v_0, and the integration can be done explicitly. For the phonon-branch minimum, the contribution of the scattering by defects appears only in the region $\omega^2 > \omega_0^2$:

$$\Gamma(\omega) = \Gamma^{nat} + \frac{c_d}{4\pi\omega_0 s^3} |v_0|^2 \sqrt{\omega^2 - \omega_0^2}. \quad (2)$$

In the case of the phonon-branch maximum, we have the disorder contribution only if $\omega^2 < \omega_0^2$.

Expression (2) has a transparent physical meaning: the phonon elastic scattering from defects produces some phonon width in the frequency range where the appropriate final phonon states occur. For instance, in the case of the minimum of the phonon branch at $\omega = \omega_0$, the final phonon states occur only for $\omega > \omega_0$. Of course, this effect manifests itself as a line asymmetry in the Raman light scattering on phonons. As a result, the high-frequency wing of the line drops more slowly (than the low-frequency one) for a phonon branch having the minimum at the center of the Brillouin zone.

We emphasize that the frequency dependence of the phonon width is determined by the dimensionality of defects. As we see from Eq. (2), this is a square-root dependence for point defects. In the case of linear defects, such as dislocations (or the plane defects, e.g., crystallite boundaries or stacking faults), we have the two-dimensional (or one-dimensional) integration in Eq. (1), which gives

$$\Gamma(\omega) = \Gamma^{nat} + \frac{c_l}{4\omega_0 s^2} |v_0|^2 \theta(\omega^2 - \omega_0^2) \quad (3)$$

for line defects and

$$\Gamma(\omega) = \Gamma^{nat} + \frac{c_p}{4\omega_0 s} |v_0|^2 (\omega^2 - \omega_0^2)^{-1/2} \quad (4)$$

for plane defects, where c_l and c_p are concentrations of line and plane defects, respectively and $\theta(x)$ is the Heaviside step function.

The singularities in Eqs. (3) and (4) and a weak singularity in Eq. (2) arise because the width of final states was not taken into account. There is another shortcoming of the simple expressions (1)–(4): they do not describe the shift of the phonon frequency due to the interaction with disorder. Therefore, we have to use a more complicated technique of the Green's functions [14].

The heart of the technique is the phonon self-energy

$$\Sigma(\omega) = -c_d \sum_k \frac{|v(\mathbf{k} - \mathbf{q})|^2}{\Omega^2(\omega) \pm s^2 k^2 - i\omega\Gamma(\omega) - \omega^2}. \quad (5)$$

The real functions $\Omega(\omega)$ and $\Gamma(\omega)$ are now themselves defined by the real and imaginary parts of the self-energy. We obtain them by solving the system of the equations

$$\Omega^2(\omega) - \omega_0^2 - i\omega[\Gamma(\omega) - \Gamma^{nat}] - c_d v(q = 0) = \Sigma(\omega). \quad (6)$$

The last term (named the homogenous shift) in the left-hand side of Eq. (6) gives the phonon shift due to the averaged effect of disorder, whereas the self-energy, Eq. (5), describes the fluctuation effect of the defects. In addition to the phonon shift (inhomogeneous, depending on the frequency), the self-energy produces a phonon width. We note that if the phonon does not interact with disorder ($v = 0$), Eqs. (6) naturally give $\Omega(\omega) = \omega_0$ and $\Gamma(\omega) = \Gamma^{nat}$. Next, in the Born approximation, Eqs. (5) and (6) give the simple expression, Eq. (1), for phonon damping.

In the Raman light scattering, the wave-vector transfer $q \sim \omega^{(i)}/c$ is determined by the wave vector of incident light, $\omega^{(i)}$ being the incident light frequency. In integral (5), the values of $k \sim 1/l = \sqrt{\Gamma\omega_0}/s$ are important, where l plays the role of the phonon mean free path. The dispersion parameter $s \approx 5 \cdot 10^5$ cm/s is typically of the order of the sound velocity and the width Γ is of the order of $(10^{-2}–10^{-1})\omega_0$. Thus, the condition $q \ll k$ holds and we can omit q in Eq. (5).

To simplify the calculations, we assume that the potential function $v(\mathbf{k})$ takes a constant value v_0 in the region $k < 1/r_0$ and is equal to zero for $k > 1/r_0$. Then the parameter r_0 gives the size of the region in the real space where phonons are scattered by defects. If we consider phonon scattering by strain fluctuations, r_0 has the meaning of the correlation length of these fluctuations.

The line asymmetry is very sensitive to the relation between the parameters r_0 and l. The case where $r_0 < l$

is referred to as the short-range disorder. It is easy to verify that the line asymmetry is much larger for the short-range disorder than in the opposite case. We can rewrite the condition of the short-range disorder as

$$\pi \frac{r_0 \sqrt{\Gamma\omega_0}}{a\omega_D} < 1 \quad (7)$$

using the estimate of the Debye frequency $\omega_D = \pi s/a$, where a is the lattice constant.

For point defects, the calculation of $\Sigma(\omega)$, Eq. (5), gives

$$\Sigma(\omega) = A \left[b - (a_1 - ia_2) \left(\frac{1}{4} \ln \frac{(b + a_1)^2 + a_2^2}{(b - a_1)^2 + a_2^2} + \right. \right.$$
$$\left. \left. + \frac{i}{2} \arctan \frac{b + a_1}{a_2} + \frac{i}{2} \arctan \frac{b - a_1}{a_2} \right) \right] \quad (8)$$

in the case of the phonon branch maximum and

$$\Sigma(\omega) = A \left[-b + (a_2 + ia_1) \left(\frac{1}{4} \ln \frac{(b + a_2)^2 + a_1^2}{(b - a_2)^2 + a_1^2} - \right. \right.$$
$$\left. \left. - \frac{i}{2} \arctan \frac{b + a_2}{a_1} - \frac{i}{2} \arctan \frac{b - a_2}{a_1} \right) \right] \quad (9)$$

in the case of the photon branch minimum. Here,

$$a_1 = \sqrt{\frac{1}{2}[\Omega^2(\omega) - \omega^2 + \rho(\omega)]},$$

$$a_2 = \sqrt{\frac{1}{2}[-\Omega^2(\omega) + \omega^2 + \rho(\omega)]},$$

$$\rho(\omega) = \sqrt{(\Omega^2(\omega) - \omega^2)^2 + \omega^2\Gamma^2(\omega)},$$

$$b = s/r_o, \quad A = c_d v_0^2/2\pi^2 s^3.$$

We note that the dimensions are the following: s in cm$\cdot[\omega]$, c_d in cm^{-3}, v_0 in cm$^3 \cdot [\omega^2]$, and A in $[\omega]$.

Solving the system of Eqs. (5) and (6), we find the functions $\Omega(\omega)$ and $\Gamma(\omega)$. We can then calculate (e.g., see [4]) the Raman intensity

$$I(\omega) \sim \frac{1}{1 - \exp(-\hbar\omega/k_B T)} \times$$
$$\times \frac{\omega\Gamma(\omega)}{(\Omega^2(\omega) - \omega^2)^2 + \omega^2\Gamma^2(\omega)}. \quad (10)$$

Equation (10) can be applied to the Stokes lines ($\omega > 0$) as well as to the anti-Stokes ones ($\omega < 0$).

If $\Omega(\omega) = \omega_0$ and $\Gamma(\omega) = \Gamma^{nat}$ are constant, Eq. (10) gives the Lorentzian line shape, because $\Gamma^{nat} \ll \omega_0$. But, as we have already seen, the non-Lorentzian line shape is obtained if the width $\Gamma(\omega)$ depends on ω.

Up to this point, we have considered a single phonon line. In the general case, there are several lines with their positions $\Omega_i(\omega)$ and widths $\Gamma_i(\omega)$. The corresponding terms have to be summed in Eq. (10). The intervalley terms with v_{ij} could also be written in self-energy (5). These terms are essential when the disorder removes the degeneration of branches.

3. COMPARISON OF THE THEORY WITH THE EXPERIMENTAL DATA FOR ZIRCONIA

Two Raman spectra taken from paper [5] are shown in Fig. 1. They were recorded from two samples of yttria-stabilized (8.6 mol. % of $YO_{1.5}$) zirconia: the first in the as-deposited condition (bottom) and the second (top) annealed at $1200\,^{\circ}C$. Narrowing and decrease of the asymmetry of the lines are evident. The fit to the theory, Eqs. (8) and (9), is shown by solid lines; parameters of the fit are listed in the Table. In fitting, we assume that the effect of disorder on the spectra from the sample after annealing is negligible ($A = 0$). There is no information about the width of Raman lines for pure zirconia. Therefore, the line widths for the sample after annealing are referred to as the natural widths Γ^{nat}.

The broadening $\Gamma - \Gamma^{nat}$ of the line for the sample in as-deposited conditions is induced by the phonon–disorder interaction determined by the parameter A. We assume that the natural width Γ^{nat} of each line be-
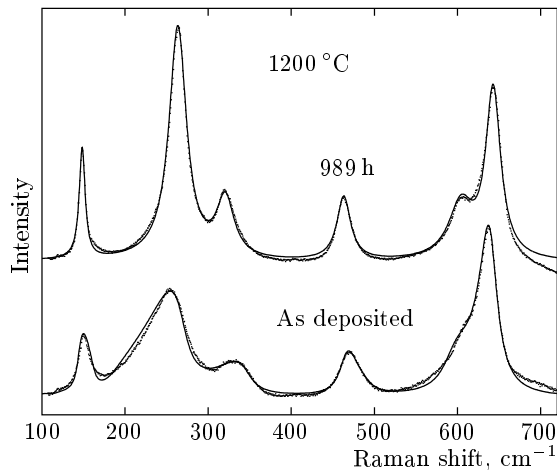
Fig. 2. The Raman line $470\ cm^{-1}$ (points correspond to the experiment data [5], solid lines to the theory) from the sample in as-deposited conditions (left panel, bottom) and after annealing for 989 h at $1200\ ^{\circ}C$ (left panel, top); the peak of the line from the as-deposited sample is marked by the vertical dash-dotted lines. The asymmetry of the line indicates that the phonon branch has a minimum. In the right panel, the total width $\Gamma(\omega)$ (top) and the inhomogeneous shift $\Omega(\omega) - \omega_0$ (bottom) are plotted versus the Raman shift for two spectra

fore annealing is equal to Γ^{nat} of the same line after annealing (see the Table).

The line shape of spectra for the sample with disorder is determined by two factors: (i) the value of the parameter r_0 and (ii) the extremum type (minimum or maximum) of the phonon branch. In Figs. 2 and 3, the results of fitting are shown in detail. The $470.5\ cm^{-1}$ line is shown in Fig. 2, left panel. The high-frequency wing of the line from the as-deposited sample is more gentle. This corresponds to the minimum of the phonon branch. In the right panel, the width $\Gamma(\omega)$ and the inhomogeneous shift $\Omega(\omega) - \omega_0$ are plotted at the top and bottom, respectively, as functions of the Raman shift ω. For the sample after annealing, they are constant: $\Gamma(\omega) = \Gamma^{nat}$ and $\Omega(\omega) = \omega_0$.

We see that the width $\Gamma(\omega)$ of the line from the as-deposited sample increases with the frequency transfer around the line peak Ω_0, which is marked by the dash-dotted vertical line. This resembles the square-root dependence in Eq. (2) for the minimum of the phonon branch, and we use Eq. (9) in fitting. At the peak position, the width takes the value Γ_0; this value is given in Table, it is slightly less than the FWHM (full-width at half-maximum) because of the frequency dependent

Fig. 1. Raman spectra (points correspond to the experiment data [5], solid lines to the theory) for a sample in as-deposited conditions (bottom) and after annealing for 989 h at $1200\,^{\circ}C$ (top)
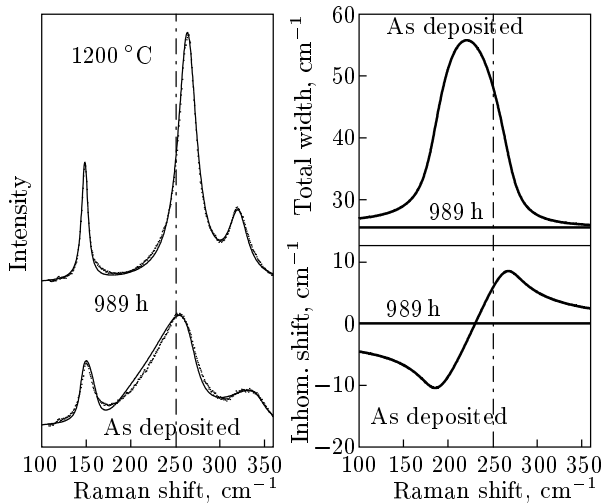
Fig. 3. The same as in Fig. 2, but for the line $250\ cm^{-1}$. The phonon branch now has the maximum

line width function $\Gamma(\omega)$.

The behavior of the $250\ cm^{-1}$ line (see Fig. 3) from the as-deposited sample has the opposite character: the low-frequency wing drops more slowly. Then we use Eq. (8) corresponding to the maximum of the phonon branch. The asymmetry parameter As listed in Table is the difference between the right and left wings at the half-maximum. This parameter takes positive (negative) values for the phonon-branch minimum (maximum). The asymmetry parameter and the FWHM were determined for the line extracted from the total spectra with the help of the fit.

Several points can be noted in Table. First, the radius of defects (correlation radius) is about the value of the lattice parameter a. This is the case of a short-range disorder resulting in the evident asymmetry of the line shape. Second, because of disorder, the line position is slightly shifted (by less than 5 %), but the line width increases considerably. This can be understood with the help of Figs. 2 and 3 (right panels). The frequency dependence of the shift function $\Omega(\omega) - \omega_0$ has a zero about the line peak, whereas the width function $\Gamma(\omega)$ takes almost its maximum value.

4. DISCUSSION

Lughi and Clarke [5] explained their results in the following way. The Raman line becomes more symmetric after annealing. According to condition (7), this means that the correlation radius of disorder in as-deposited samples must be quite small, of a few lattice

parameters. Therefore, the disorder cannot be induced by large-scale strain fluctuations, for instance, of the crystallite size (about 50 nm).

The disorder with a small correlation length can be realized by Y^{3+} ions and their associated oxygen vacancies. But the concentration of yttria (8.6 mol. %) before and after annealing is the same in the sample. Lughi and Clarke [5] proposed a redistribution mechanism of the Y^{3+} ions and oxygen vacancies. They reasoned that the regions of the c phase become richer (and the t phase is more pure) in the Y^{3+} ions and oxygen vacancies in the $t - c$ phase transformation during annealing. Because of this redistribution of defects, the Raman-active t phase exhibits symmetric and narrowing Raman lines.

Considering the ions and vacancies as point defects that scatter the long-wave optical phonons, we use Eqs. (8) and (9) in our comparison.

Finally, as can be seen from Table, the phonon–disorder interaction is larger for lower frequency lines. This interaction decreases progressively with the frequency of the lines. We conclude that the distribution of the heavier defect ions, i.e., Y^{3+}, affects the phonon modes stronger than the disorder of oxygen vacancies.

REFERENCES

1. A. Göbel, T. Ruf, J. M. Zhang, R. Lauck, and M. Cordona, Phys. Rev. B **59**, 2749 (1999).

2. S. Nakashima, Y. Nakatake, H. Harima, M. Katsuno, and N. Ohtani, Appl. Phys. Lett. **77**, 3612 (2000); S. Nakashima, H. Ohta, M. Hangyo, and B. Palosz, Phil. Mag. B **70**, 971 (1994).

3. S. Rohmfeld, M. Hundhausen, and L. Ley, Phys. Rev. B **58**, 9858 (1998).

4. L. A. Falkovsky, J. M. Bluet, and J. Camassel, Phys. Rev. B **55**, R14697 (1997); **57**, 11283 (1998).

5. V. Lughi and D. R. Clarke, J. Amer. Ceram. Soc. **88**, 2552 (2005).

6. P. W. Anderson and E. I. Blount, Phys. Rev. Lett. **14**, 217 (1965).

7. J. Cai, C. Raptis, Y. S. Raptis, and E. Anastassakis, Phys. Rev. B **51**, 201 (1995).

8. Y. Ishibashi and V. Dvorak, J. Phys. Soc. Jpn. **58**, 4211 (1989).

9. K. Negita and H. Takato, J. Phys. Chem. Sol. **50**, 325 (1989).

10. A. P. Migorodsky, M. B. Smirnov, and P. E. Quintard, Phys. Rev. B **55**, 19 (1997).

11. S. Fabris, A. T. Paxton, and M. W. Finnis, Phys. Rev. B **61**, 6617 (2000).

12. E. Anastassakis, B. Papanicolaou, and I. M. Asher, J. Phys. Chem. Sol. **36**, 667 (1975).

13. P. Bouvier, H. C. Gupta, and G. Lucazeau, J. Phys. Chem. Sol. **62**, 873 (2001).

14. L. A. Falkovsky, Pis'ma v Zh. Eksp. Teor. Fiz. **66**, 817 (1997).

15. L. A. Falkovsky, Uspechi Fiz. Nauk **66**, 817 (2004).

16. S.-I. Tamura, Phys. Rev. B **30**, 849 (1984).